Small-molecule SUMO inhibition for biomarker-informed B-cell lymphoma therapy

Uta M. Demel,[1,2,3] Matthias Wirth,[1,2] Schayan Yousefian,[1,4,5] Le Zhang,[1,2] Konstandina Isaakidis,[1,2] Judith Dönig,[6] Marlitt Böger,[1,2] Nikita Singh,[1,2] Hazal Köse,[1,2] Simon Haas,[1,4,5,7,8,9] Stefan Müller,[6] Markus Schick[1,2] and Ulrich Keller[1,2,7]

[1]Department of Hematology, Oncology and Cancer Immunology, Campus Benjamin Franklin, Charité - Universitätsmedizin Berlin, corporate member of Freie Universität Berlin and Humboldt-Universität zu Berlin, Berlin; [2]Max-Delbrück-Center for Molecular Medicine, Berlin; [3]Clinician Scientist Program, Berlin Institute of Health (BIH), Berlin; [4]Berlin Institute of Health (BIH) at Charité – Universitätsmedizin Berlin, Berlin; [5]Berlin Institute for Medical Systems Biology, Max Delbrück Center for Molecular Medicine in the Helmholtz Association, Berlin; [6]Institute of Biochemistry II, Goethe University Frankfurt, Medical School, Frankfurt; [7]German Cancer Consortium (DKTK), German Cancer Research Center (DKFZ), Heidelberg; [8]Heidelberg Institute for Stem Cell Technology and Experimental Medicine (HI-STEM gGmbH), Heidelberg and [9]Division of Stem Cells and Cancer, Deutsches Krebsforschungszentrum (DKFZ) and DKFZ-ZMBH Alliance, Heidelberg, Germany

Correspondence: Ulrich Keller
ulrich.keller@charite.de

Received: March 7, 2022.
Accepted: September 13, 2022.
Prepublished: September 22, 2022.

https://doi.org/10.3324/haematol.2022.280995

Small molecule SUMO inhibition for biomarker-informed B-cell lymphoma therapy

Demel et al.

SUPPLEMENTARY METHODS

Transcriptome profiling and processing of gene expression data

Transcriptome data from human DLBCL patient samples was downloaded from the gene expression omnibus (GEO) database as CEL files of datasets GSE98588 and GSE34171[1 2]. Gene expression data of DLBCL cell lines, which were experimentally divided into SUMOi-responder cells (Oci-LY19, SU-DHL-5, SU-DHL-8) and SUMOi-non-responder cells (U-2932, SU-DHL-4, DB, NU-DHL-1) was accessed via the GEO accession number GSE53798[3]. Transcriptome data from murine *Eμ-Myc* induced lymphomas and healthy B-cells was accessed via GSE7897[4]. The CEL files of the Affymetrix Human Genome U133 arrays or Affymetrix Mouse Genome 430 2.0 arrays were processed using Expression Console software (Affymetrix). Data was normalized using the robust multi-array algorithm (RMA), log2 transformed and probes were collapsed. Z-scores were generated from the expression matrices and identifiers of the SUMO core machinery were used for further cluster analyses. *SUMO1, SUMO2, SUMO3, UBA2,* and *SAE1* identifiers were used to generate the $SUMO^{high}$ and $SUMO^{low}$ clusters within the GSE98588 dataset. Accordingly, $SUMO^{high}$ and $SUMO^{low}$ clusters were generated within the GSE34171 dataset, including canonical MYC targets (*ODC1*, *NCL*, *CAD*, *MYC).* Clinical data was used for survival analysis visualized by Kaplan-Meier plots. Statistical comparison of the two survival curves was performed using a log-rank test. Hierarchical clustering was performed according to the Euclidean distance and Ward method for both columns and rows using ClustVis software[5]. The resulting unbiased dichotomization into the two main groups $SUMO^{low}$ and $SUMO^{high}$ was used to subject the respective samples to gene set enrichment analysis of log2 transformed data. For the GSEA of the DLBCL cell lines as well as the transcriptome data of the *Eμ-myc* lymphomas, log2 transformed expression values were used. The respective groups from the used datasets were analyzed using GeneTrail3.0 software (Kolgomorov-Smirnov test)[6] and the Hallmark and Reactome gene signatures from the Molecular Signature Database (MSigDb)[7]. The generated results were graphically visualized in a volcano plot or in a GSEA plot, generated with GraphPadPrism software v9. Within the *Eμ-myc* dataset, the SUMO core machinery identifiers

were used for principal component analysis (PCA). The PCA plot was generated using ClustVis software[5].

Single Cell RNA-seq analysis

Quality assessment of scRNA-seq data. For this part of the study, we used the publicly available CITE-seq dataset of SUMOi treated C57Bl6 mice (GSE193359). Count matrices were imported into R (version 4.1.0) and processed with the Seurat package (4.0.5). Cells with >=200 detected genes and containing <10% mitochondrial reads were retained for further analysis. Outlier cells were removed by applying upper filtering thresholds for the number of genes and UMIs which were set to >=6,000 and >=40,000, respectively. Moreover, genes captured in <3 cells were removed from the count matrix. Samples were demultiplexed based on the HTO expression and only singlets were included in subsequent analyses. HTO demultiplexing was performed using Seurat's HTODemux function with default parameters. A preliminary clustering of non-integrated data was conducted and signature genes for each cluster were determined using Seurat's FindMarker function. Cell populations that co-expressed marker genes for distinct cell types, were defined as doublet clusters and removed prior to data integration. Additionally, to remove contamination of ambient RNA in single cells, decontX[8] was independently applied for each batch with default parameters. The decontaminated count matrices were used for all downstream analyses.

Data integration, clustering and cell type annotation. Following quality assessment and selection of high-quality cells, samples were integrated to remove batch effects. For this, Seurat's standard integration workflow was applied. Initially, decontaminated RNA counts were log-normalized to account for library size differences and the top 2,000 variable genes were determined. Subsequently, integration features were determined, and integration anchors selected using CCA (canonical correlation analysis) and mutual nearest neighbors (MNN) [9]. After integration, the object was scaled, and a principal component analysis (PCA) performed. The top 30 principal components were selected for shared nearest neighbor (SNN) graph construction, clustering (using the Louvain algorithm) and UMAP visualization. To find

signature genes for each cluster, Seurat's FindMarker function was applied. Spleen cell populations were manually annotated based on knowledge-derived gene lists and marker genes. B cells from both conditions were subsetted and reclustered using the top 20 PCs as described above.

Differential abundance analysis. DA-seq[10] was applied to identify differentially abundant B cell populations between the conditions. The analysis was performed based on the instructions in the DA-seq tutorial (on https://klugerlab.github.io/DAseq/articles/tutorial.html) with values for k ranging from 20 to 500. As DA-seq does not provide any statistical output, a differential abundance testing of B cell clusters was conducted using mouse-wise pseudobulks. In brief, cell numbers for each sample (mouse) and cluster were determined. In the next step, the cell type frequencies were calculated for each population and sample by dividing the respective cell number by the total number of cells within that cluster. To determine statistical significance, design and contrast matrices were generated using the model.matrix (stats package version 4.1.0) and makeContrasts function (limma package version 3.48.1). The glmFit function (edgeR package version 3.34.0) was used to fit a Negative Binomial Generalized Linear Model and likelihood ratio tests were performed using glmLRT (edgeR package).

Sumo-Myc correlation analysis. Given the comparatively high degree of sparsity in single-cell RNA-seq data, the following analysis used module scores for Sumo and Myc expression, respectively. To generate these gene scores, Seurat's AddModuleScore function was utilized. The *Sumo* score consisted of the six SUMO core machinery genes: *Sumo1*, *Sumo2*, *Sumo3*, *Sae1*, *Uba2*, *Ube2i*. For the *Myc* score, the "hallmark *Myc* targets V2" gene list was used (https://www.gsea-msigdb.org). The AddModuleScore function was run independently for each condition and the mean score expression per cluster and condition was calculated. Mean expression values were then scaled from 0-1 (condition-wise) by applying a min-max scaling (highest expression value = 1, lowest expression value 0). The scaled mean expression values of both scores were plotted against each other for each cell population and the Pearson correlation coefficient (R) was calculated using the stat_cor function (ggpubr package 0.4.0). In addition, we studied how SUMOi treatment would affect the correlation of Sumo and Myc

module scores. To do so, the correlation (R) between Sumo and Myc scores were calculated for each population condition-wise. Cell cluster with <50 cells in one of the conditions were excluded from this analysis.

Analysis of cell proliferation. The expression of a cell proliferation score was used to assess whether certain cell populations are more proliferative active. The proliferation score was generated with Seurat's AddModuleScore function using genes from the GSEA gene set "cell_proliferation_GO_0008283".

SUPPLEMENTARY REFERENCES

1. Chapuy B, Stewart C, Dunford AJ, et al. Molecular subtypes of diffuse large B cell lymphoma are associated with distinct pathogenic mechanisms and outcomes. Nat Med. 2018;24(5):679-690.
2. Monti S, Chapuy B, Takeyama K, et al. Integrative analysis reveals an outcome-associated and targetable pattern of p53 and cell cycle deregulation in diffuse large B cell lymphoma. Cancer Cell. 2012;22(3):359-372.
3. Falgreen S, Dybkaer K, Young KH, et al. Predicting response to multidrug regimens in cancer patients using cell line experiments and regularised regression models. BMC Cancer. 2015;15:235.
4. Mori S, Rempel RE, Chang JT, et al. Utilization of pathway signatures to reveal distinct types of B lymphoma in the Emicro-myc model and human diffuse large B-cell lymphoma. Cancer Res. 2008;68(20):8525-8534.
5. Metsalu T, Vilo J. ClustVis: a web tool for visualizing clustering of multivariate data using Principal Component Analysis and heatmap. Nucleic Acids Res. 2015;43(W1):W566-570.
6. Gerstner N, Kehl T, Lenhof K, et al. GeneTrail 3: advanced high-throughput enrichment analysis. Nucleic Acids Res. 2020;48(W1):W515-W520.
7. Liberzon A, Birger C, Thorvaldsdottir H, Ghandi M, Mesirov JP, Tamayo P. The Molecular Signatures Database (MSigDB) hallmark gene set collection. Cell Syst. 2015;1(6):417-425.
8. Yang S, Corbett SE, Koga Y, et al. Decontamination of ambient RNA in single-cell RNA-seq with DecontX. Genome Biol. 2020;21(1):57.
9. Stuart T, Butler A, Hoffman P, et al. Comprehensive Integration of Single-Cell Data. Cell. 2019;177(7):1888-1902 e1821.
10. Zhao J, Jaffe A, Li H, et al. Detection of differentially abundant cell subpopulations in scRNA-seq data. Proc Natl Acad Sci U S A. 2021;118(22)

SUPPLEMENTARY MATERIAL

Antibodies

Epitope	Reactivity	Flurochrome	Company	Catalogue number
B220	mouse	PE-Cy7	Invitrogen	25-0452-82
B220	mouse	APC-Cy7	Invitrogen	47-0452-82
CD3e	mouse	PE-Cy5.5	Invitrogen	35-0031-82
CD4	mouse	PE-Cy7	Invitrogen	25-0041-82
CD8a	mouse	PE	BD	553032
CD19	mouse	eFluor450	eBioscience	48-0193-82
CD21/35	mouse	PE	BD	552957
CD23	mouse	PE-Cy7	Invitrogen	25-0232-82
CD25	mouse	FITC	Invitrogen	56-0251-82
CD44	mouse	FITC	Invitrogen	11-0441-82
CD62L	mouse	eFluor450	Invitrogen	48-0621-82
CD69	mouse	eFluor450	Invitrogen	48-0691-82
CD80	mouse	PE	eBioscience	12-0801-81
CD86	mouse	PE-Cy5/PerCP	Invitrogen	15-0862-81
CD127	mouse	APC	Invitrogen	17-1271-82
Foxp3	mouse	PE	eBioscience	12-5773-82
IgD	mouse	eFluor450	Invitrogen	48-5993-82
IgM	mouse	APC	Invitrogen	15-5790-82
MHC-II	mouse	APC-Cy7	eBioscience	47-5321-82
DAPI	all	-	Biolegend	422801
PI Solution	all	-	Sigma	25535-16-4

Westernblot Antibodies

Target	Company	Article number
MYC	Cell signaling	9402S
β-Tubulin	DSHB	E7

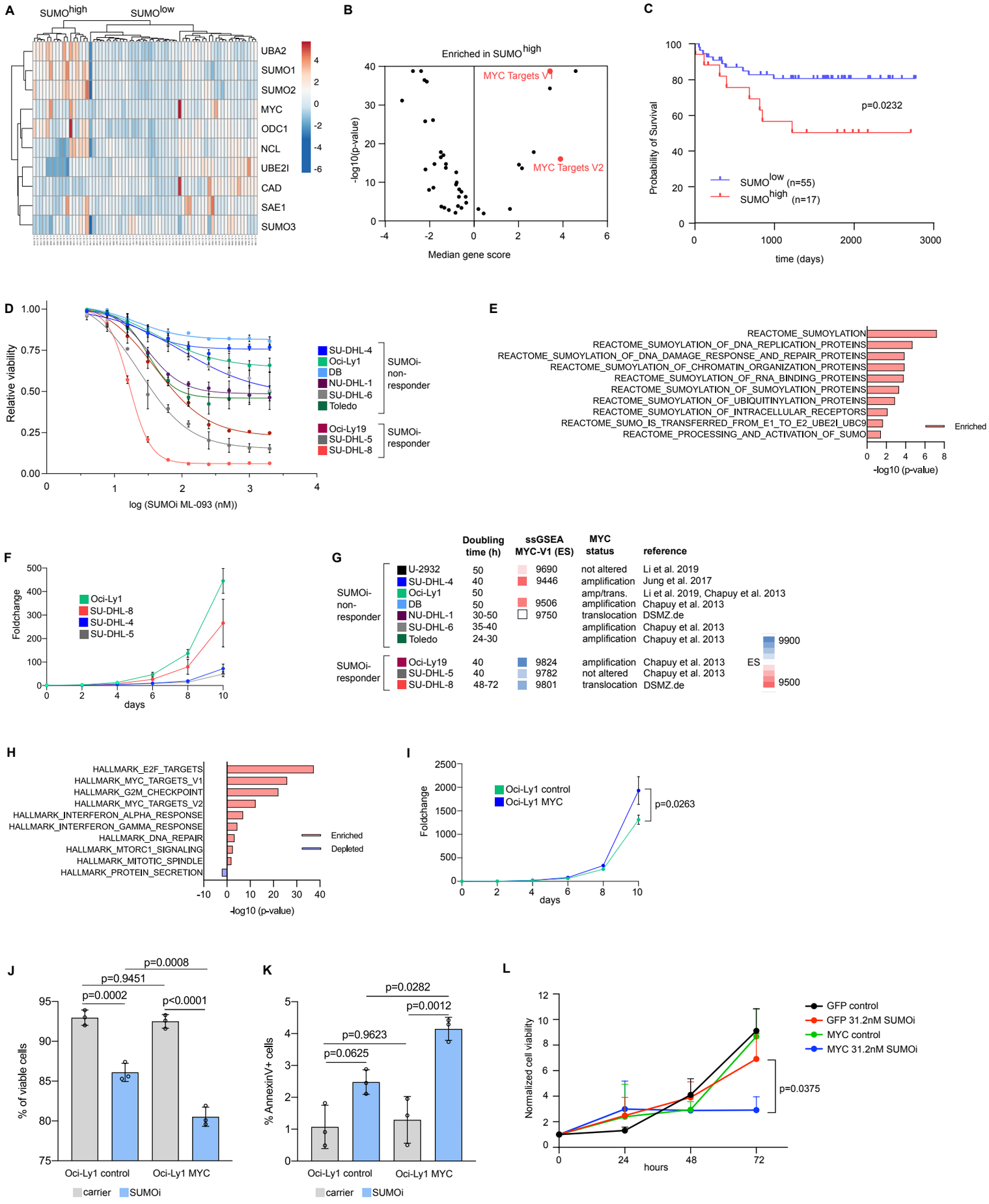

Supplementary Figure S1

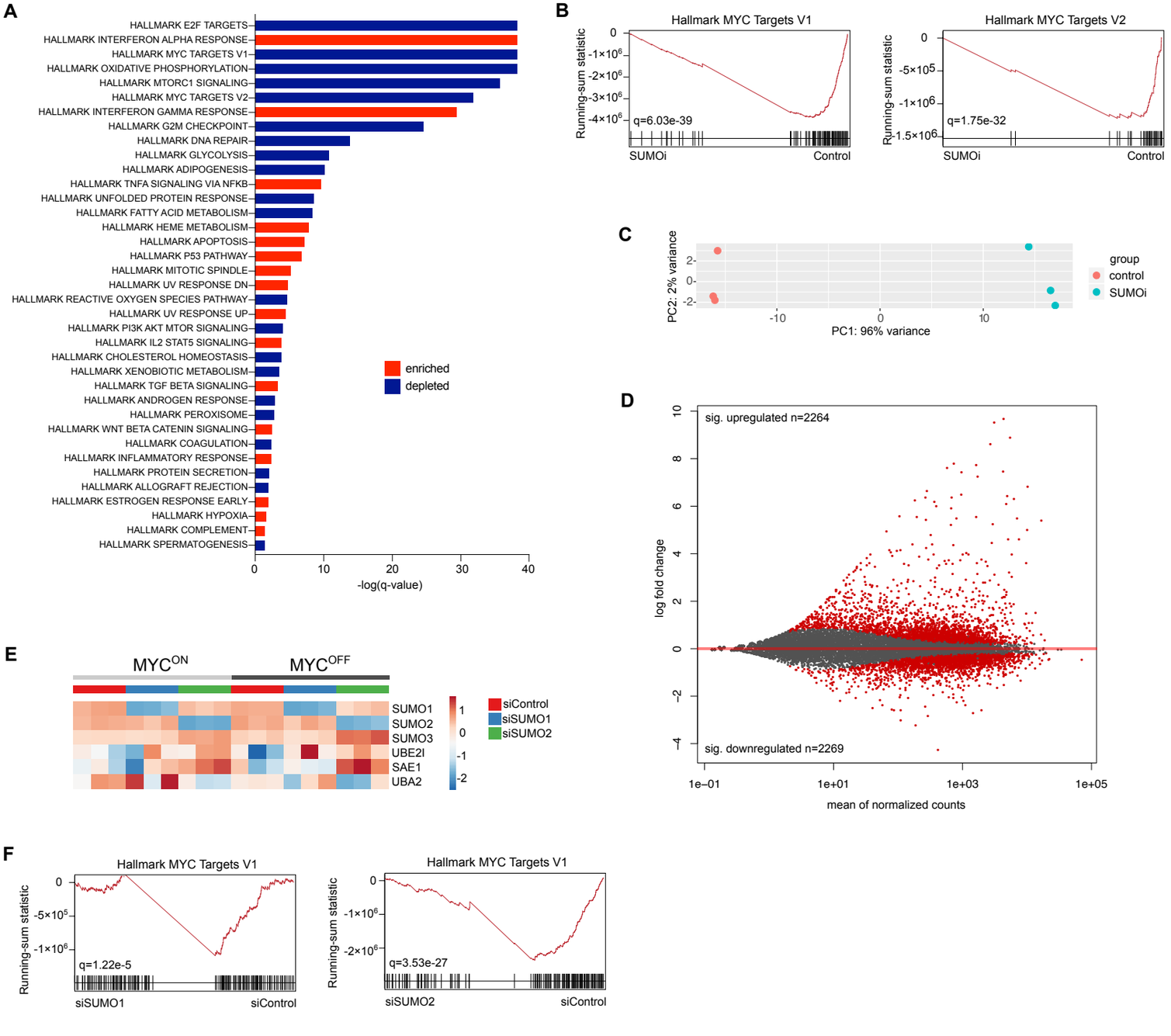

Supplementary Figure S2

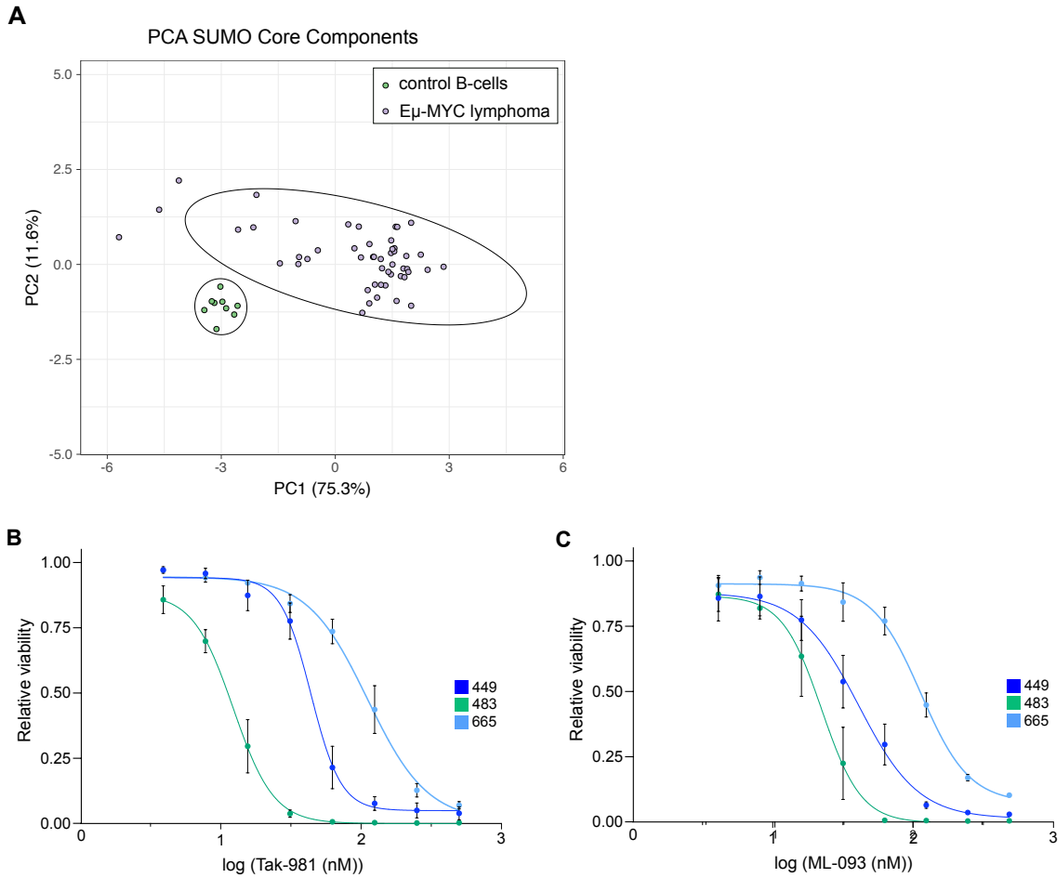

Supplementary Figure S3

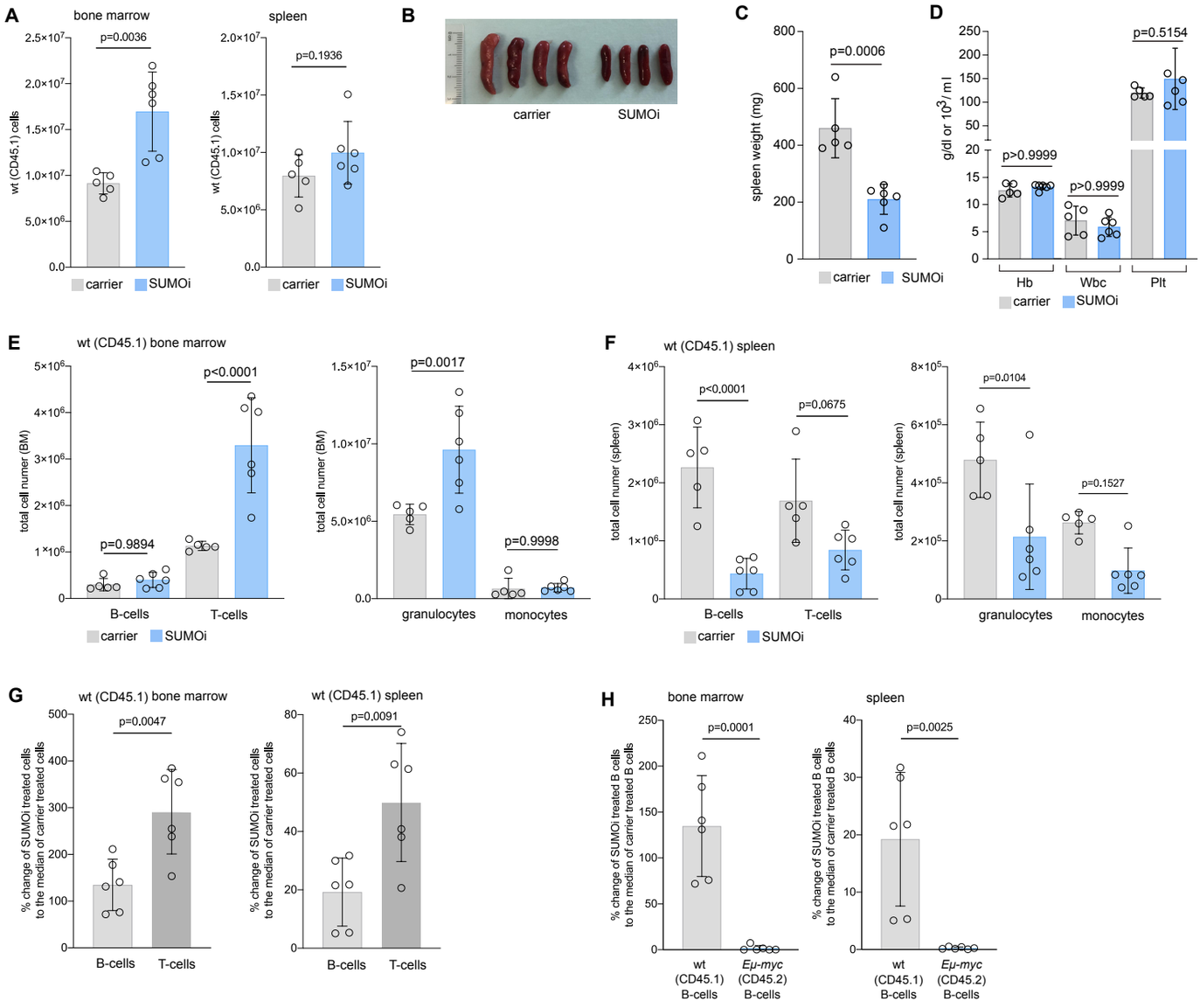

Supplementary Figure S4

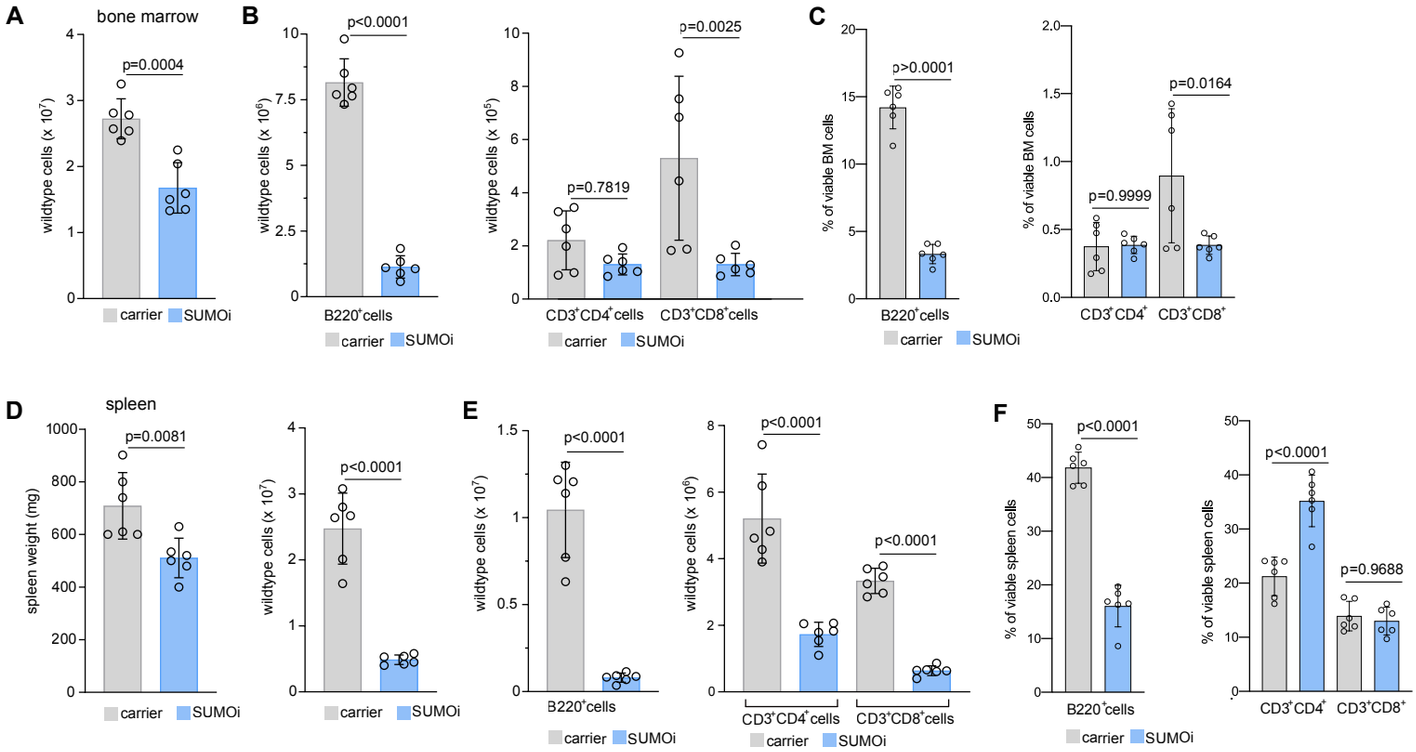

Supplementary Figure S5

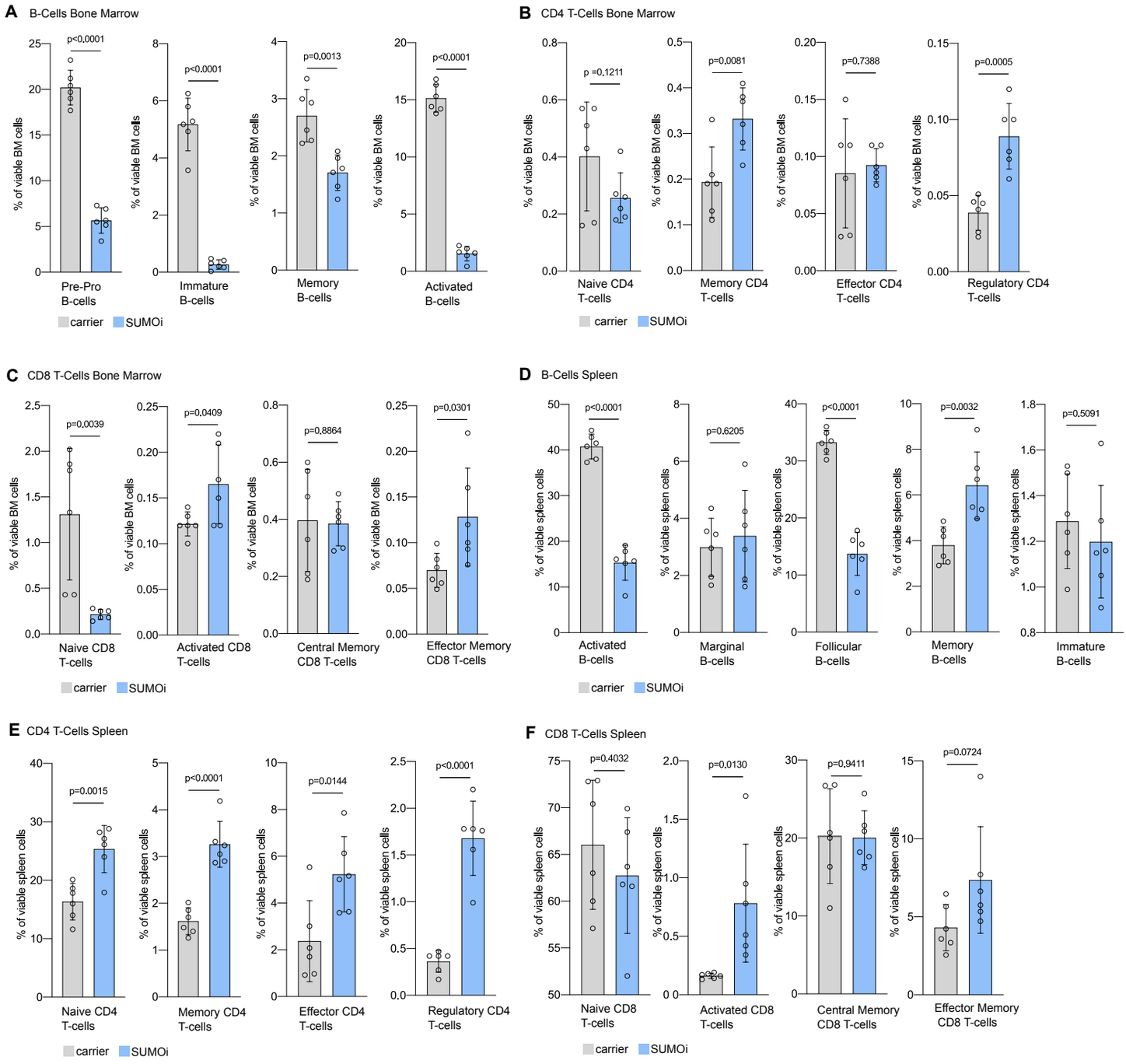

Supplementary Figure S6

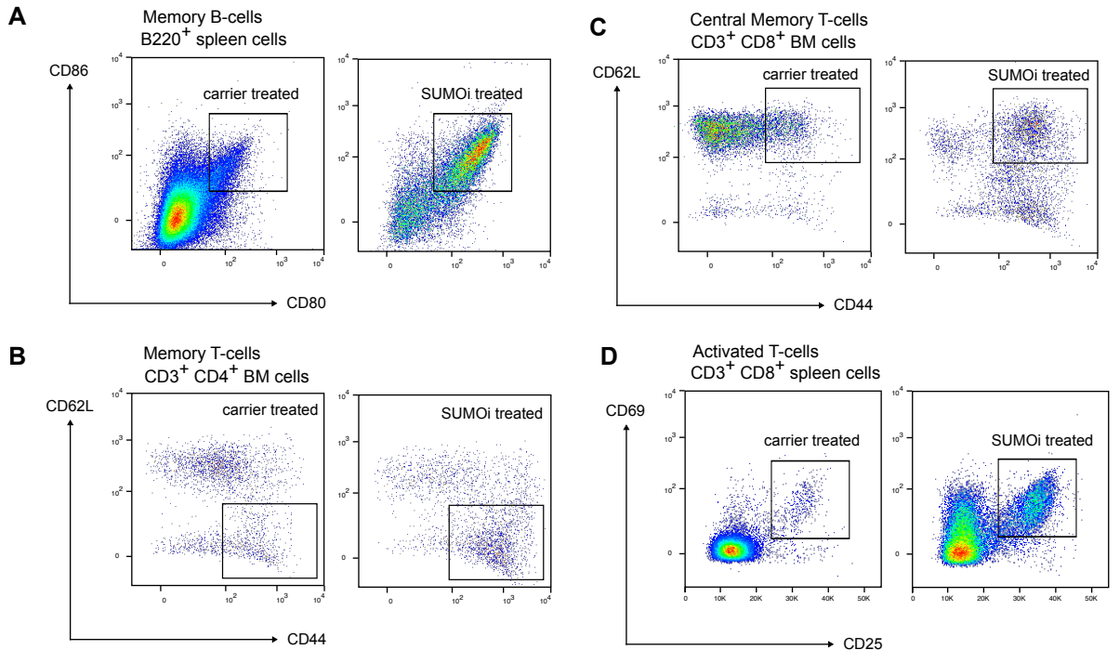

Supplementary Figure S7

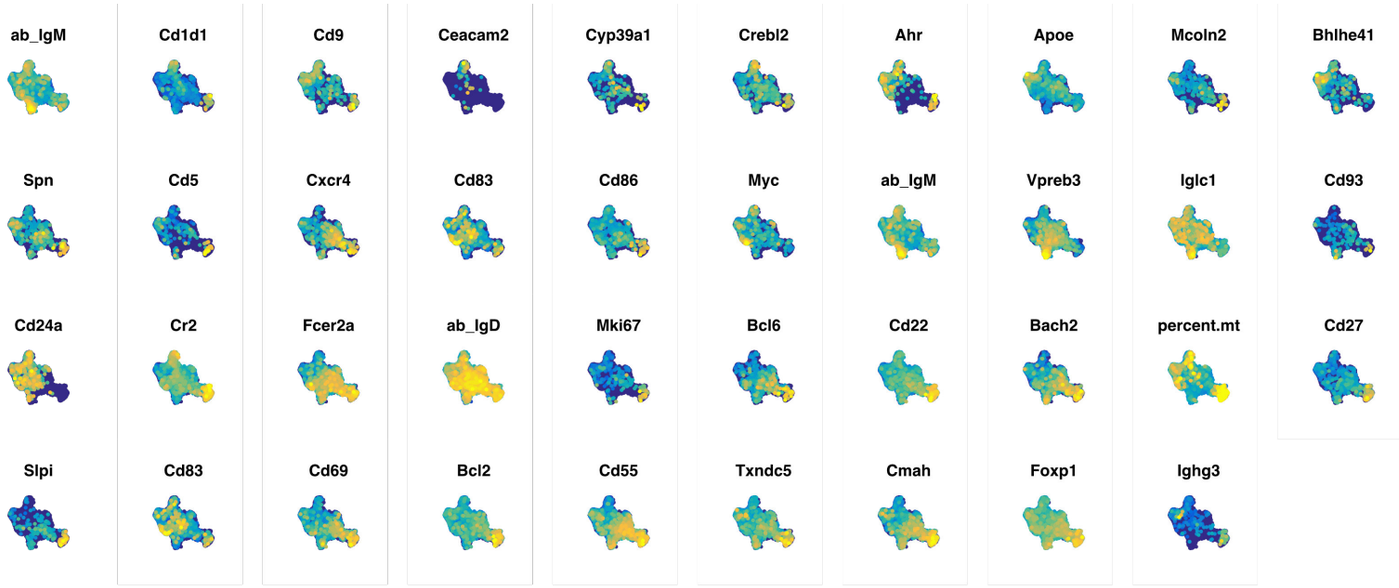

Supplementary Figure S8

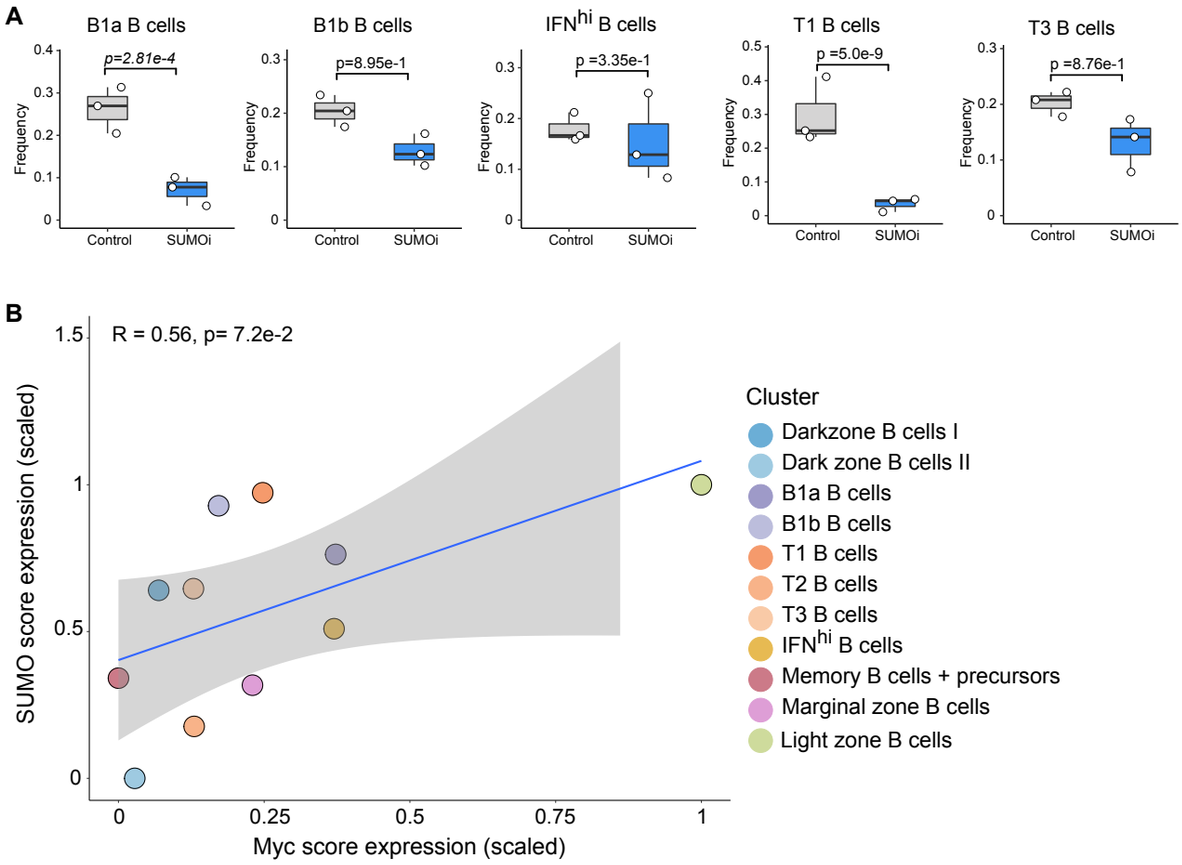

Supplementary Figure S9

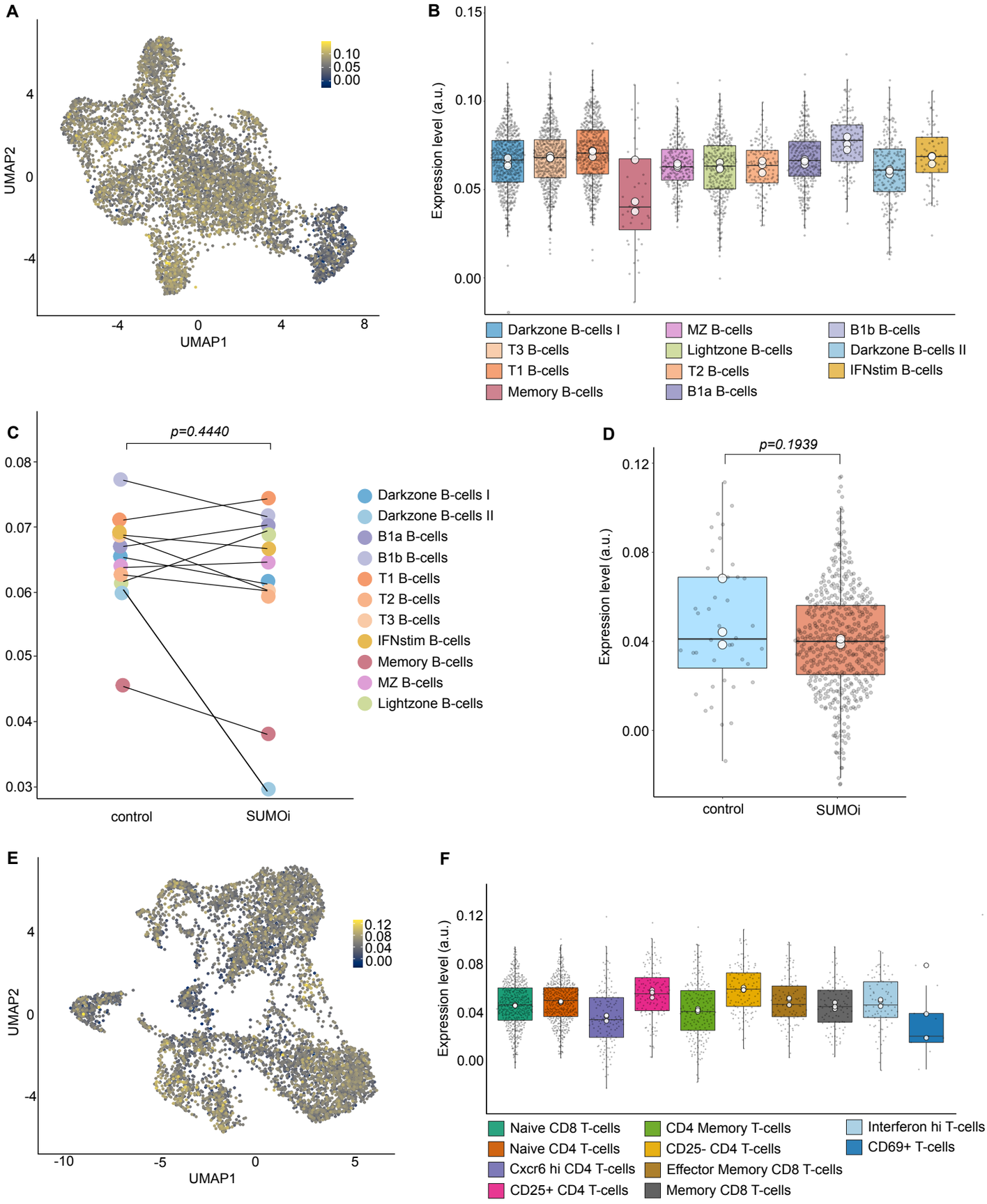

Supplementary Figure S10

SUPPLEMENTARY FIGURE LEGENDS

Supplementary Figure S1.

A) Hierarchical clustering (Euclidean/Ward) of indicated SUMO core components, MYC, and MYC target genes of normalized human DLBCL transcriptome profiles (GSE34171) revealed $SUMO^{high}$ and $SUMO^{low}$ subgroups as indicated.
B) Gene set enrichment analysis of $SUMO^{high}$ and $SUMO^{low}$ subgroups identified in (A). Volcano plot displays significant gene signatures of the Hallmark gene set (MSigDb) with both MYC Hallmark signatures (v1, v2) highlighted.
C) Kaplan-Meier-Plot of DLBCL patients from the GSE34171 dataset. Patient survival has been dichotomized based on the clustering method displayed in (A). Log rank p-value is indicated.
D) Flow cytometry analysis of relative viability of indicated DLBCL cell lines treated with increasing SUMOi concentrations (ML-093, 0, 3.9, 7.8, 15.6, 31.2, 62.5, 125, 250, 500, 1000, 2000nM) for 72h (n=3).
E) Gene set enrichment analysis of SUMOi-responder (Oci-Ly19, SU-DHL-5, SU-DHL-8) vs. SUMOi-non-responder (U-2932, SU-DHL-4, DB, NU-DHL-1) on expression profiles accessed via GSE53798. Bar plot of enriched SUMOylation signatures, obtained from Reactome knowledgebase.
F) Analysis of cell proliferation of two SUMOi non-responder cell lines and two SUMOi-responder cell lines.
G) Table displaying doubling-time, MYC status and ssGSEA MYC-V1 enrichment score of each cell line. ssGSEA enrichment score representing the expression of genes in the MYC-V1 data set.
H) Bar plot displaying top 10 enriched/depleted gene signatures of the Hallmark gene set (MSigDb) within SUMOi-responding and SUMOi-non-responding cells as described in (D).
I) Analysis of cell proliferation of Oci-Ly1 cells transduced with a MYC expression plasmid or a control plasmid. P-value refers to cell proliferation on day 10 and is determined by unpaired t-test.
J) Flow cytometric analysis of cell death of Oci-Ly1 cells transduced with a MYC expression plasmid or control plasmid, treated with control or SUMOi (Tak-981, 31.2nM, 72h, n=3)
K) Flow cytometric analysis of apoptosis of Oci-Ly1 cells transduced with a MYC expression plasmid or control plasmid, treated with control or SUMOi (Tak-981, 31.2nM, 72h, n=3).
L) Oci-Ly1 cells transduced with MYC plasmid or control plasmid were treated with SUMOi (Tak-981, 31.2nM) and cell viability was measured by CellTiterGlo after 0, 24, 48 and 72h (n=3).

Supplementary Figure S2.

A) Summary of GSEA of expression data derived from transcriptome profiling Oci-Ly1 cells treated with control or SUMOi (400nM, 48h) with the indicated gene sets. P-value determined by Kolmogorov-Smirnov test.
B) Transcriptome analysis of RNAseq data from Oci-Ly1 cells, treated with the SUMOi Tak-981 (400nM, 48h) revealed significant negative enrichments for both MYC hallmark gene sets. FDR-q values are indicated.

C) Principal Component Analysis (PCA) of transcriptome profiles of Oci-Ly1 cells, treated with control or SUMOi (400nM, 48h).
D) MA plot visualizing differentially expressed genes (DEG) and their average expression. Significant genes were defined as all genes with an adj.p-value < 0.05. Here, n=2264 could be determined as significantly upregulated and n=2269 as significantly downregulated.
E) U2OS-MYC^{tetON} cells were seeded and simultaneously transfected with *SUMO1, SUMO2* and control siRNAs. 42h after transfection cells were treated with either doxycyclin (MYC^{on}) or a vehicle control (MYC^{off}). After a total of 72h cells were harvested, RNA was isolated and analyzed by RNAseq. Heatmap indicates normalized mRNA expression levels of the SUMO core components SUMO1, SUMO2, SUMO3, SAE1, UBA2 and UBE2I.
F) Enrichment plots of Hallmark MYC targets V1 indicating significant negative enrichments in U2OS-MYC^{on} SUMO1 or SUMO2 knockdown cells (as described in Fig.S2E). FDR-q values are indicated.

Supplementary Figure S3.

A) Transcriptome data from murine *Eμ-Myc* induced lymphomas and healthy B-cells was accessed via GSE7897. The SUMO core machinery components Sumo1, Sumo2, Sumo3, Ube2i, Uba2, Sae1 have been used for principal component analysis (PCA).
B) Flow cytometry analysis of relative viability of indicated murine Eμ-Myc lymphoma cell lines treated with increasing SUMOi concentrations (0, 3.9, 7.8, 15.6, 31.2, 62.5, 125, 250, 500, 1000, 2000nM) for 72h (n=3) using Tak-981.
C) Flow cytometry analysis of relative viability of indicated murine Eμ-Myc lymphoma cell lines treated with increasing SUMOi concentrations (0, 3.9, 7.8, 15.6, 31.2, 62.5, 125, 250, 500, 1000, 2000nM) for 72h (n=3) using ML-093.

Supplementary Figure S4.

A) Total number of wild-type (wt, CD45.1) cells in the bone marrow (BM) and spleen after carrier vs. SUMOi treatment (ML-093, 50mg/kg). N=6, p-values was determined by unpaired t-test.
B) Picture of representative spleens of *Eμ-myc* lymphoma mice after carrier vs. SUMOi treatment (treatment scheme outlined in Fig. 2A).
C) Spleen weight following SUMOi treatment. N=6, *p-value* was determined by unpaired t-test.
D) Analysis of hemoglobin (Hb), white blood cells (Wbc) and platelets (Plt) after carrier vs. SUMOi treatment. *P-values* were determined by ANOVA; Tukey`s post hoc test.
E) Total number of wt (CD45.1) B-cells (B220^{+}), T-cells (CD3^{+}), granulocytes (Gr. 1^{+}CD11b^{+}) and monocytes (Gr.1^{+}CD11b^{+}) in the BM following SUMOi treatment compared to carrier. N=6, P-values were determined by ANOVA; Tukey`s post hoc test.
F) Total number of wt (CD45.1) B-cells (B220^{+}), T-cells (CD3^{+}), granulocytes (Gr. 1^{+}CD11b^{+}) and monocytes (Gr.1^{+}CD11b^{+}) in the spleen following SUMOi treatment compared to carrier. N=6, P-values were determined by ANOVA; Tukey`s post hoc test.
G) Relative change of SUMOi-treated B-cells and T-cells cells to the median number of the respective carrier-treated cell population in BM and spleen. N=6, p-values was determined by unpaired t-test.

H) Relative change of SUMOi-treated B-cells to the median number of carrier-treated B-cells, calculated for wt and Eμ-myc B-cells in BM and spleen. N=6, p-values was determined by unpaired t-test.

Supplementary Figure S5.

A) Total number of BM cells after carrier vs. SUMOi treatment, as outlined in Fig. 3A. N=6, p-value was determined by unpaired t-test.
B) Total number of indicated cell populations (B220+ B-cells, CD3+CD4+ T-cells, CD3+CD8+ T-cells) in the BM after carrier vs. SUMOi treatment. N=6, p-values were determined by unpaired t-test.
C) Relative number of indicated cell populations (B220+ B-cells, CD3+CD4+ T-cells, CD3+CD8+ T-cells) of viable BM cells after carrier vs. SUMOi treatment. N=6, p-values were determined by unpaired t-test.
D) Spleen weight and total number of spleen cells after carrier vs. SUMOi treatment for 48h. N=6, p-values were determined by unpaired t-test.
E) Total number of indicated cell populations (B220+ B-cells, CD3+CD4+ T-cells, CD3+CD8+ T-cells) in the spleen after carrier vs. SUMOi treatment. N=6, p-values were determined by unpaired t-test.
   Relative number of indicated cell populations (B220+ B-cells, CD3+CD4+ T-cells, CD3+CD8+ T-cells) of viable spleen cells after carrier vs. SUMOi treatment. N=6, p-values were determined by unpaired t-test.

Supplementary Figure S6.

A) Relative number of indicated B220+ BM cell populations (B220+IgM- Pre-Pro B-cells, B220+IgM+IgD- Immature B-cells, B220+CD80+CD86+ Memory B- cells, B220+CD19+MHC-II+ Activated B-cells) of viable BM cells after carrier vs. SUMOi treatment. N=6, p-values were determined by unpaired t-test.
B) Relative number of indicated CD3+CD4+ BM cell populations (CD3+CD4+CD44lowCD62L+ Naïve T-cells, CD3+CD4+CD44highCD62L- Memory T-Cells, CD3+CD4+CD44lowCD62L- Effector T-cells, CD3+CD4+CD25+CD69+FoxP3+ Regulatory T-cells) of viable BM cells after carrier vs. SUMOi treatment. N=6, p-values were determined by unpaired t-test.
C) Relative number of indicated CD3+CD8+ BM cell populations (CD3+CD8+CD44lowCD62L+ Naïve T-cells, CD3+CD8+ CD44highCD62L- Effector Memory T- Cells, CD3+CD8+CD44highCD62L+ Central Memory T-cells, CD3+CD8+CD25+CD69+ Activated T-cells) of viable BM cells after carrier vs. SUMOi treatment. N=6, p-values were determined by unpaired t-test.
D) Relative number of indicated B220+ spleen cell populations (B220+CD93+ Immature B-cells, B220+CD21highCD23low Marginal zone B-cells, B220+CD21lowCD23high Follicular B-cells, B220+CD80+CD86+ Memory B-cells, B220+CD19+MHC-II+ Activated B-cells) of viable spleen cells after carrier vs. SUMOi treatment. N=6, p-values were determined by unpaired t-test.
E) Relative number of indicated CD3+CD4+ spleen cell populations (CD3+CD4+CD44lowCD62L+ Naïve T-cells, CD3+CD4+CD44highCD62L- Memory T-Cells, CD3+CD4+CD44lowCD62L- Effector T-cells, CD3+CD4+CD25+CD69+FoxP3+ Regulatory T-cells) of viable spleen cells after carrier vs. SUMOi treatment. N=6, p-values were determined by unpaired t-test.
F) Relative number of indicated CD3+CD8+ spleen cell populations (CD3+CD8+CD44lowCD62L+ Naïve T-cells, CD3+CD8+CD44highCD62L- Effector

Memory T-Cells, CD3+CD8+ CD44highCD62L+ Central Memory T-cells, CD3+CD8+CD25+CD69+ Activated T-cells) of viable spleen cells after carrier vs. SUMOi treatment. N=6, p-values were determined by unpaired t-test.

Supplementary Figure S7.

A) Scheme indicating gating strategy for Memory B-cells ($B220^{+}CD80^{+}CD86^{+}$) in the spleen after carrier vs. SUMOi treatment, as indicated in Fig. 3A.
B) Representative FACS plots illustrating gating strategy for Memory T-cells ($CD3^{+}CD4^{+}CD44^{high}CD62L^{-}$) in the BM after carrier vs. SUMOi treatment.
C) Scheme indicating gating strategy for $CD3^{+}CD8^{+}$ Central Memory T-cells ($CD3^{+}CD8^{+}CD44^{high}CD62L^{+}$) in the BM after carrier vs. SUMOi treatment.
D) Representative FACS plots illustrating gating strategy for Activated T-cells ($CD3^{+}CD8^{+}CD25^{+}CD69^{+}$) in the spleen after carrier vs. SUMOi treatment.

Supplementary Figure S8.

A) Featureplots of B cell marker genes that were used to annotate the B cell populations. Yellow = high expression; Blue = low expression

Supplementary Figure S9.

A) Differential abundance analysis on mouse-wise pseudobulks (indicated by white dots, n=3). Bar plots represent the subpopulation frequencies stratified by condition. The median is indicated by the center line of the box plot. The box extends from the 25^{th} to 75^{th} percentiles, whisker length reaches from minimum to maximum. Significance is determined by a Negative Binomial Generalized Linear Model.
B) SUMO and MYC score correlation analysis in SUMOi treated mice. Scaled mean expression values are plotted against each other for each subpopulation identified in Fig. 5B. R indicates the Pearson correlation coefficient. The regression line is shown in blue. The grey area indicates the 95% confidence interval.

Supplementary Figure S10.

A) UMAP of control and SUMOi treated B cells with highlighted expression of the proliferation module score.
B) Expression level of the proliferation score in control B cell subsets. Grey dots represent the individual cells. The back line indicates the median across all cells. White dots represent the median score expression per mouse-wise pseudobulk.
C) Pairwise comparison of the mean proliferation score expression in B cell populations. Significance was tested using a paired t-test.
D) Expression level of the proliferation score in memory B-cells. A two-sided Wilcoxon rank sum test was applied to determine significance. Grey dots indicate the individual cells. The back line represents the median across all cells. White dots indicate the median score expression per mouse-wise pseudobulk.
E) UMAP of control and SUMOi treated T cells with highlighted expression of the proliferation module score.
F) Expression level of the proliferation score in control T cell subsets. Grey dots represent the individual cells. The back line indicates the median across all cells. White dots represent the median score expression per mouse-wise pseudobulk.